

# Lunar and Solar Daily Variations in the Earth Current at Kakioka, Japan

by

Masanori SHIRAKI

## Abstract

Hourly values of earth current potential gradient observed at Kakioka, Japan, for the period 1962–1973, have been analysed to determine the lunar and solar daily variations in the earth current. The results for these variations in the earth current are compared with each other. These results are also compared with the lunar and solar daily variations in the geomagnetic field at the same observatory for the same period.

## 1. Introduction

The lunar daily variation ( $L$ ) in the geomagnetic field is quite definitely established. This variation at Kakioka and other two observatories in Japan has recently been determined and discussed by the present author (Shiraki, 1977). Because of the close connection between earth current and geomagnetic field, lunar daily variation in the earth current is also expected. Really it has already been found by Yokouchi (1939) at Kakioka. However, the amount of data used in his analysis is of only two years and is not enough for the precise determination of  $L$ . Moreover the relation between  $L$  in the geomagnetic field and that in the earth current at this observatory has not been examined as yet.

It is therefore of interest to reanalyse the lunar daily variation in the earth current at Kakioka from a large amount of data (12 years from 1962 to 1973). The result for the lunar daily variation has been compared with that for the solar daily variation ( $S$ ) which can be obtained at the same time as a byproduct. Moreover, the lunar and solar daily variations in the geomagnetic field at the same observatory have been analysed for the same period by the same method, too, and the relation between earth current and geomagnetic field has been examined and discussed briefly.

## 2. Analysis

If  $(l_n, \lambda_n)$  and  $(s_n, \sigma_n)$  are the amplitude and phase of  $n$ -th harmonic for  $L$  and  $S$  variations, respectively, one may write,

$$L = \sum L_n = \sum l_n \sin(nt - 2\nu + \lambda_n) \quad (1)$$

$$S = \sum S_n = \sum s_n \sin(nt + \sigma_n) \quad (2)$$

where  $t$  is the local mean solar time and  $\nu$  is the age of the mean moon. Usually, by the method of Chapman and Miller (1940), the first four harmonics for  $S$  and  $L$  are simultaneously determined from hourly values of earth current or of geomagnetic field. Their vector probable errors are also calculated by the manner described by Malin and Chapman (1970).

Earth current at Kakioka has been observed as the potential gradient between two electrodes of the span of about 1 km in a direction  $5^\circ$  west of north and its rectangular direction. These two components are temporarily designated as  $N'$  and  $E'$ , respectively. The hourly values for each of  $N'$  and  $E'$  components were first analysed as a whole and then reanalysed after subdivision into three Lloyd's seasons; winter (January, February, November and December), equinox (March, April, September and October) and summer (May, June, July and August). Any days on which data are incomplete have been omitted from the analysis. The percentage of such days to total ones is 2.7% for  $N'$  component and 2.3% for  $E'$  component. To compare  $L$  (or  $S$ ) in earth current with that in geomagnetic field as precisely as possible in later discussions, results of the analysis for  $N'$  and  $E'$  components are converted into those for the geographic components; northward component  $N$  and eastward component  $E$ . The results of the analysis for  $N$  and  $E$  components are given in Table 1

Table 1. Lunar harmonics in the earth current potential gradient at Kakioka.  
Unit: 0.01  $mv/km$ .

	$l_1$	p.e.	$\lambda_1$	$l_2$	p.e.	$\lambda_2$	$l_3$	p.e.	$\lambda_3$	$l_4$	p.e.	$\lambda_4$
Northward component $N$												
all	13	6	148	13	3	78	14	2	123	5	2	350
winter	55	15	194	41	8	59	15	5	194	7	4	42
equinox	11	3	54	12	3	136	17	3	92	7	2	314
summer	28	5	64	9	3	231	24	3	109	6	2	332
Eastward component $E$												
all	27	14	106	124	9	299	55	5	95	15	6	331
winter	197	27	217	182	14	324	73	11	136	22	7	342
equinox	46	14	43	105	16	288	50	13	66	4	7	338
summer	188	24	58	117	15	273	68	11	75	18	11	314

Table 2. Solar harmonics in the earth current potential gradient at Kakioka.  
Unit: 0.1  $mv/km$ .

	$s_1$	$\sigma_1$	$s_2$	$\sigma_2$	$s_3$	$\sigma_3$	$s_4$	$\sigma_4$
Northward component $N$								
all	6	293	18	208	11	44	2	264
winter	10	244	14	186	8	19	3	204
equinox	7	295	20	206	15	38	5	240
summer	9	354	21	224	13	66	4	338
Eastward component $E$								
all	44	282	52	174	27	349	3	127
winter	50	244	35	167	25	305	13	110
equinox	50	290	61	181	39	349	11	160
summer	49	312	62	172	30	25	12	318

for *L* and in Table 2 for *S*, respectively. It is noted that the potential gradient is expressed in millivolt per kilometer (*mv/km*) and the current flow in the *N* (*E*) component is reckoned positive when the flow is towards the north (east) and negative when in the opposite sense.

Moreover, the hourly mean values for declination *D*, horizontal intensity *H* and vertical intensity *Z* of the geomagnetic field at Kakioka have been analysed for the same interval as that of the data of earth current by the same method, too. The number of missing days is three for *Z* at the most. The results of the analysis for *D* and *H* also have been converted into those for the geographic components of the field; north component *X* and east component *Y*. The results of the analysis for *X*

Table 3. Lunar harmonics in the geomagnetic field at Kakioka. Unit: 0.01  $\gamma$ .

	$l_1$	<i>p.e.</i>	$\lambda_1$	$l_2$	<i>p.e.</i>	$\lambda_2$	$l_3$	<i>p.e.</i>	$\lambda_3$	$l_4$	<i>p.e.</i>	$\lambda_4$
Northward component <i>X</i>												
all	46	16	226	82	7	71	54	3	234	9	4	95
winter	129	26	275	134	12	100	69	7	259	17	5	99
equinox	59	22	161	53	12	47	44	10	205	4	5	359
summer	53	35	171	92	16	43	63	10	227	12	8	110
Eastward component <i>Y</i>												
all	34	8	90	101	4	295	45	4	109	14	3	302
winter	20	14	269	121	7	8	53	5	208	18	4	18
equinox	31	17	110	91	9	286	53	6	90	31	5	266
summer	91	14	83	203	10	265	98	9	89	14	6	305
Vertical component <i>Z</i>												
all	29	7	194	34	4	286	37	3	250	9	3	88
winter	53	10	43	86	7	222	40	6	321	15	3	137
equinox	45	9	204	44	6	308	44	5	226	13	4	22
summer	88	11	205	63	7	355	62	6	232	13	5	92

Table 4. Solar harmonics in the geomagnetic field at Kakioka. Unit: 0.1  $\gamma$ .

	$s_1$	$\sigma_1$	$s_2$	$\sigma_2$	$s_3$	$\sigma_3$	$s_4$	$\sigma_4$
Northward component <i>X</i>								
all	21	58	43	328	30	141	7	339
winter	31	351	26	292	23	96	9	297
equinox	32	74	61	329	43	142	14	332
summer	28	99	48	346	34	169	8	70
Eastward component <i>Y</i>								
all	111	28	95	213	62	30	19	223
winter	34	37	40	195	45	14	27	202
equinox	119	28	97	207	78	26	31	220
summer	178	26	152	222	66	46	11	306
Vertical component <i>Z</i>								
all	69	89	38	318	32	160	11	350
winter	54	75	31	301	28	135	14	322
equinox	71	88	41	319	39	156	18	344
summer	84	98	45	330	34	185	8	63

and  $Y$  components are presented in Table 3 for  $L$  and in Table 4 for  $S$  together with the results for  $Z$  component.

In Tables 2 and 4 the vector probable errors for  $S$  harmonics are not given because they are very small in comparison with the amplitudes and they are very close to the vector probable errors for the corresponding  $L$  harmonics in Tables 1 and 3.

### 3. Discussions

The amplitude  $I_n$  or  $s_n$  is considered to be significant at the five percent level when it exceeds 2.08 times its vector probable error (Leaton, Malin and Finch, 1962). Using this criterion, all  $S$  harmonics in Tables 2 and 4 are significant. For  $L$  harmonics all but 4 out of 32 determinations in Table 1 and all but 5 out of 48 determinations in Table 3 are significant.

Figs. 1 and 2 show the smoothed  $L$  and  $S$  variations of earth current, respectively. Such variations (called daygraphs) are drawn from synthetic hourly values derived from Eq. (1) or (2) using harmonic coefficients in Table 1 or 2, respectively. The daygraphs in Fig. 1 refer to the epoch of new moon and are drawn as if the sun

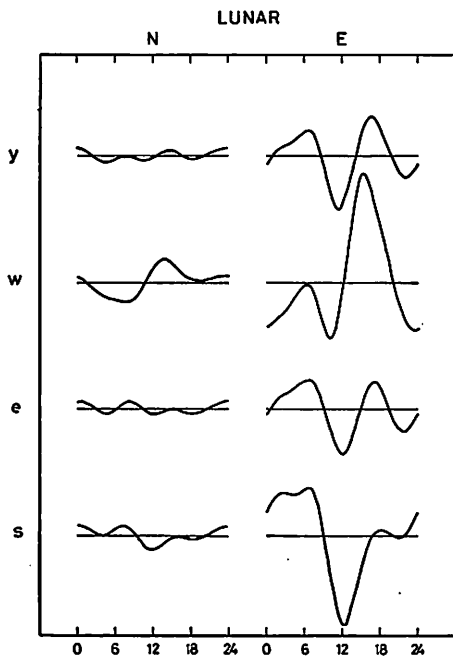


Fig. 1. Daygraphs for the annual (y) mean and seasonal (w: winter, e: equinox, s: summer) mean lunar daily variations of  $N$  and  $E$  components in the earth current potential gradient at Kakioka. The curves refer to the epoch of new moon.

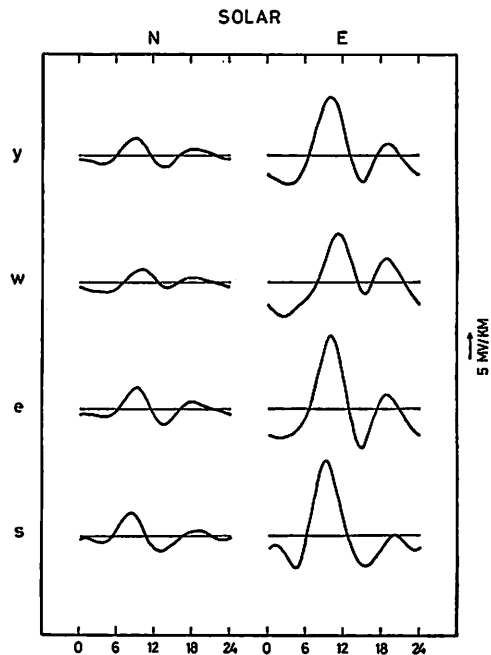


Fig. 2. Daygraphs for the annual (y) mean and seasonal (w: winter, e: equinox, s: summer) mean solar daily variations of  $N$  and  $E$  components in the earth current potential gradient at Kakioka.

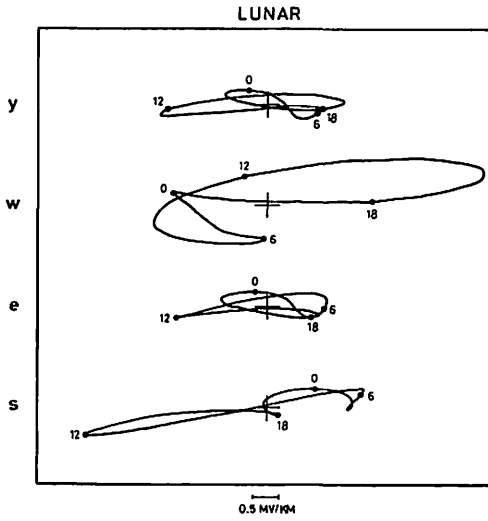


Fig. 3. Horizontal vector diagrams for the annual (y) mean and seasonal (w: winter, e: equinox, s: summer) mean lunar daily variations in the earth current potential gradient at Kakioka. The curves refer to the epoch of new moon.

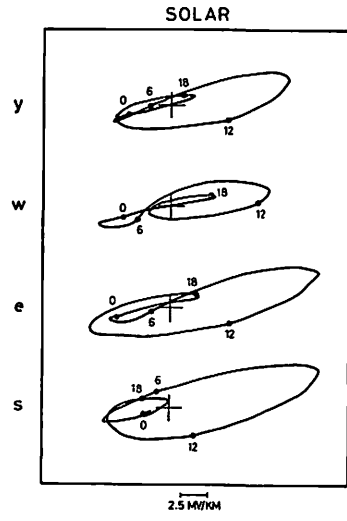


Fig. 4. Horizontal vector diagrams for the annual (y) mean and seasonal (w: winter, e: equinox, s: summer) mean solar daily variations in the earth current potential gradient at Kakioka.

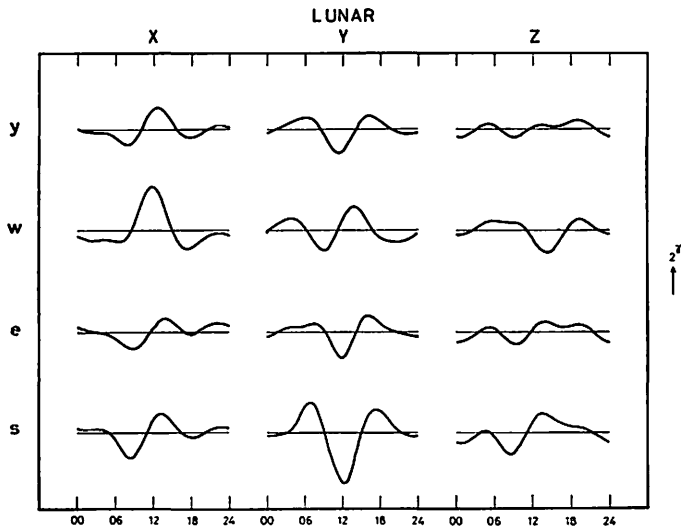


Fig. 5. Daygraphs for the annual (y) mean and seasonal (w: winter, e: equinox, s: summer) mean lunar daily variations of X, Y and Z components at Kakioka. The curves refer to the epoch of new moon.

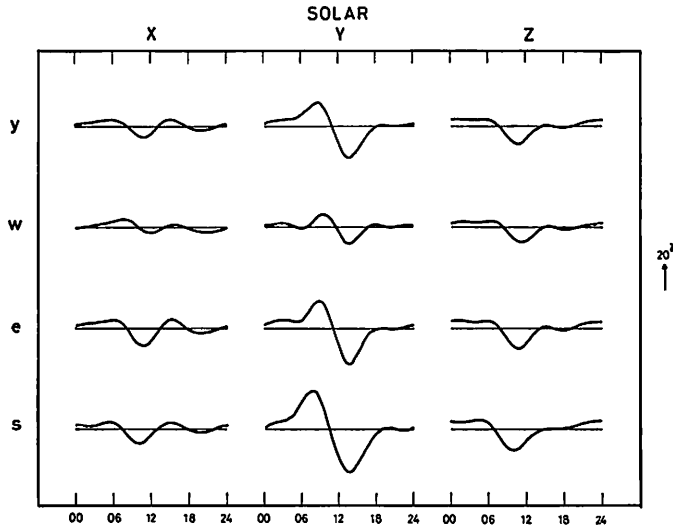


Fig. 6. Daygraphs for the annual (y) mean and seasonal (w: winter, e: equinox, s: summer) mean solar daily variation of X, Y and Z components in the geomagnetic field at Kakioka.

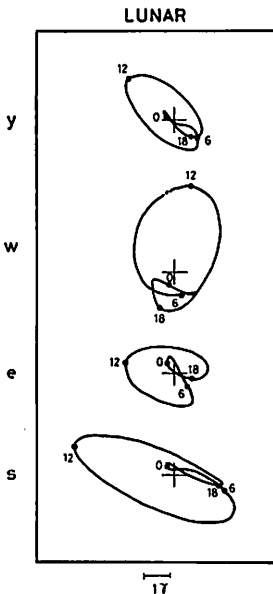


Fig. 7. Horizontal vector diagrams for the annual (y) mean and seasonal (w: winter, e: equinox, s: summer) mean lunar daily variations in the geomagnetic field at Kakioka. The curves refer to the epoch of new moon.

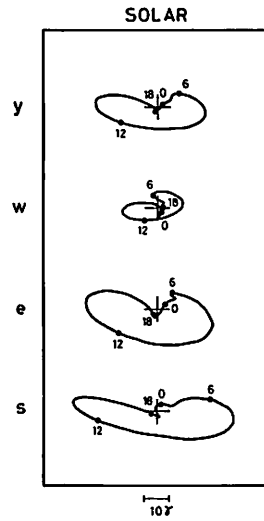


Fig. 8. Horizontal vector diagrams for the annual (y) mean and seasonal (w: winter, e: equinox, s: summer) mean solar daily variations in the geomagnetic field at Kakioka.

and the moon remained on the same meridian during the lunar day centered at new moon. In another way *L* and *S* variations may be illustrated in Figs. 3 and 4, respectively, by the horizontal vector diagrams, too, combining the daygraphs of *N* and *E* components. Similarly the daygraphs and the horizontal vector diagrams for the geomagnetic field are shown in Figs. 5–8 corresponding to Figs. 1–4, respectively.

It is clear from Figs. 1 and 2 that the range of *N* component is much smaller than that of *E* component for both *L* and *S* variations. Consequently the vector diagrams in Figs. 3 and 4 are greatly elongated in the east-west direction. Such a restriction in direction of earth current is found often in the world and is attributed to the effect of the local geological structure. The direction of elongation is usually called the principal direction of earth current.

The seasonal change of earth current for *L* in Fig. 1 or 3 is strikingly remarkable. At first, the seasonal relation of ranges is, roughly speaking,

$$L(\text{equinox}) < L(\text{winter}) < L(\text{summer})$$

and it is very different from that of *S* seen in Fig. 2 or 4. Secondly, the type of variation for *L* also shows a remarked different seasonal change as compared with that for *S*; the type of variation for *L* in winter is rather in opposite phase to that in summer, though the type of variation for *S* changes slightly among three seasons. Such an anomalous seasonal change for *L* in the earth current is similarly clear in the geomagnetic field comparing Fig. 5 or 7 with Fig. 6 or 8, respectively. The anomalous seasonal change of range is much clearer for earth current than for geomagnetic field.

The ratio of the magnitude of *S* to that of *L* is very variable among three seasons for both earth current and geomagnetic field. This is because the seasonal changes of *L* and *S* are very different from each other. The ratios of the range of daygraph for *S* to that for *L* are given in Table 5, only for the annual mean variations which are most precisely determined. In this table the ratio for *N* (*E*) component of earth current is roughly equal to that for *Y* (*X*) component of geomagnetic field. According to the induction theory in the plane earth model of homogeneous conductivity, the horizontal component of magnetic field (*X*, *Y*) is related to the horizontal component of electric field or earth current (*N*, *E*) by the formula (Rikitake, 1966),

Table 5. Ratios of the range and the amplitude of the second harmonic for *S* to those for *L*.

Earth current			
	<i>N</i>	<i>E</i>	
ratio of range ( <i>S/L</i> )	10.2	4.86	
$s_2/l_2$	14.0	4.21	
Geomagnetic field			
	<i>X</i>	<i>Y</i>	<i>Z</i>
ratio of range ( <i>S/L</i> )	4.77	14.7	14.7
$s_2/l_2$	5.21	15.7	11.4

$$\begin{pmatrix} N \\ E \end{pmatrix} = \left( \frac{i\omega}{4\pi\sigma} \right)^{1/2} \begin{pmatrix} Y \\ -X \end{pmatrix} \quad (3)$$

where  $\omega$  is the angular frequency and  $\sigma$  is the conductivity in the earth. Therefore, the above-mentioned correlation of the values of ratio between  $X$  and  $E$  or between  $Y$  and  $N$  is approximately explained by this theory. Such a correlation is also seen for the amplitude ratios of the second harmonic of  $L$  and  $S$ ; the amplitude ratios of the second harmonic for  $S$  to that for  $L$  are given in Table 5, too. Taking this fact into consideration, it is concluded that the ratio of  $S$  to  $L$  of earth current are roughly equal to those of geomagnetic field. This conclusion does not coincide with the previous one obtained by Yokouchi (1939). His conclusion is that the ratios of earth current are much smaller than those of geomagnetic field. However, his conclusion was obtained by the comparison between the earth current at Kakioka and the geomagnetic field at other observatories, and such a comparison may be insufficient. Yokouchi reported that the amplitude ratios of the second harmonic for  $S$  to that for  $L$  show similar values for both  $N$  and  $E$  components, though in the present result the ratio for  $N$  component is much larger than that for  $E$  component. This may be explained by the reason that his determination of  $N$  component was incorrect due to the much small amplitude of variation. Moreover, the present much different values of ratio for  $N$  and  $E$  component may be explained by the reason that the relative location of Kakioka to the center of the equivalent overhead current system for  $L$  is much different from that for  $S$  (Shiraki, 1977).

Looking again at the horizontal vector diagrams of earth current in Figs. 3 and 4, it is clear that the principal direction for  $L$  is different from that for  $S$ . Because the earth current is clearly connected to the geomagnetic field as described above, it should be taken into consideration that the vector diagrams of the geomagnetic field are also somewhat elongated for both  $L$  and  $S$  in different directions. However, even after this consideration, the principal direction of earth current for  $L$  is different from that for  $S$  by about  $25^\circ$ . Such a fact is also seen when only the second harmonic of  $L$  and  $S$  is concerned. The difference of the principal directions for  $L$  and  $S$  may be attributed partly to the error of the determination of  $L$  variation, but may be mainly explained by the fact that the  $L$  variations in earth current and geomagnetic field have two parts due to the ionospheric and oceanic dynamo origin (Malin, 1970). The principal direction of the ionospheric dynamo part of  $L$  variation may be the same to the principal direction of  $S$  variation due to their same generation mechanism, but the principal direction of the oceanic dynamo part of  $L$  variation may be not necessarily the same to it.

#### Acknowledgements

The author thanks Prof. H. Maeda of Kyoto University for his interest in this study and his critical reading of the manuscript. Thanks are also due to Dr. M. Kawamura, the Director of the Kakioka Magnetic Observatory, for his encouragement.



## References

- Chapman, S. and J. C. P. Miller (1940): The Statistical Determination of Lunar Daily Variations in Geomagnetic and Meteorological Elements, *Month. Not. Roy. astr. Soc., Geophys. Suppl.*, **4**, 649-669.
- Leaton, B. R., S. R. Malin and H. F. Finch (1962): The Solar and Luni-Solar Daily Variation of the Geomagnetic Field at Greenwich and Abinger, 1916-1957, *Roy. Obs. Bull. London*, No. 63, D273-D318.
- Malin, S. R. C. (1970): Separation of Lunar Daily Geomagnetic Variations into Parts of Ionospheric and Oceanic Origin, *Geophys. J. Roy. astr. Soc.*, **21**, 447-455.
- Malin, S. R. C. and S. Chapman (1970): The Determination of Lunar Daily Geophysical Variations by the Chapman-Miller Method, *Geophys. J. Roy. astr. Soc.*, **19**, 15-35.
- Rikitake, T. (1966): *Electromagnetism and the Earth's Interior*, Elsevier, Amsterdam.
- Shiraki, M. (1977): Solar and Lunar Daily Geomagnetic Variations at Kakioka, Memambetsu and Kanoya, Japan, 1958-1973, *Geophys. Mag.*, **38**, 37-70.
- Yokouchi, Y. (1939): Lunar Diurnal Variation of the Earth Current Potential at Kakioka, *Mem. Kakioka Mag. Obs.*, **2**, 65-68 (in Japanese).

## 柿岡の地電流の太陰・太陽日変化の解析

白 木 正 規

## 概 要

柿岡で観測された1962-1973年の地電位差の毎時値を用いて、地電流の太陰・太陽日変化を解析した。そして、これらの日変化を比較し、議論した。更に、同じ期間の柿岡の地磁気の毎時値から、同じ解析方法により、地磁気の太陰・太陽日変化についても解析し、地電流の日変化と比較議論した。